

# Measurement of mitochondrial H<sub>2</sub>O<sub>2</sub> production under varying O<sub>2</sub> tensions

**Anna Stepanova, Alexander Galkin\***

*Columbia University, New York, NY, United States*

*\*Corresponding author: e-mail address: ag4003@cumc.columbia.edu*

## Chapter outline

---

<b>1</b>	<b>Definition</b> .....	<b>2</b>
<b>2</b>	<b>Rationale</b> .....	<b>2</b>
<b>3</b>	<b>Materials, equipment and reagents</b> .....	<b>4</b>
	3.1 Instrumentation.....	5
<b>4</b>	<b>Protocol</b> .....	<b>6</b>
<b>5</b>	<b>Analysis and statistics</b> .....	<b>9</b>
	5.1 Data analysis algorithm.....	11
<b>6</b>	<b>Precursor techniques</b> .....	<b>14</b>
	6.1 Preparation of components for Amplex UltraRed assay.....	14
	6.2 Preparation of calibrating H <sub>2</sub> O <sub>2</sub> solution.....	14
<b>7</b>	<b>Safety considerations and standards</b> .....	<b>15</b>
<b>8</b>	<b>Pros and cons</b> .....	<b>15</b>
<b>9</b>	<b>Alternative methods/procedures</b> .....	<b>16</b>
<b>10</b>	<b>Troubleshooting and optimization</b> .....	<b>17</b>
<b>11</b>	<b>Summary</b> .....	<b>18</b>
	<b>References</b> .....	<b>18</b>

## Abstract

Mitochondria-derived reactive oxygen species (ROS) play an important role in the development of several pathologies and are also involved in physiological signaling. Molecular oxygen is the direct substrate of complex IV of the respiratory chain, and at the same time, its partial reduction in mitochondria results in the formation of ROS, mainly H<sub>2</sub>O<sub>2</sub>. The accurate knowledge of the dependence of H<sub>2</sub>O<sub>2</sub> production on oxygen concentration is vital for the studies of tissue ischemia/reperfusion, where the relationship between oxygen availability,

## 2 Measurement of mitochondrial H<sub>2</sub>O<sub>2</sub> production

respiration, and ROS production is critical. In this chapter, we describe a straightforward and reliable protocol for the assessment of H<sub>2</sub>O<sub>2</sub> release by mitochondria at varying oxygen concentrations. This method can be used for any ROS-generating system where the effect of oxygen level on H<sub>2</sub>O<sub>2</sub> production needs to be assessed.

---

### 1 Definition

Measurements of H<sub>2</sub>O<sub>2</sub> release from isolated mitochondria at varying oxygen concentrations using respirometry and fluorescence detection.

---

### 2 Rationale

Reactive oxygen species (ROS) are recognized as highly-reactive molecules involved in various pathologic conditions promoting cell-damaging oxidative stress (Golubev, Hanson, & Gladyshev, 2018; Schieber & Chandel, 2014). Recent work has demonstrated that ROS also act as specific signaling molecules involved in apoptosis, gene expression, and redox homeostasis (see D’Autreaux & Toledano, 2007; Zuo, Zhou, Pannell, Ziegler, & Best, 2015, for reviews). Since molecular oxygen is a direct substrate of ROS, the knowledge of the relationship between oxygen level and the rate of ROS production is of great importance for understanding the interplay between oxygen availability and ROS-generation in situ. Several intracellular organelles, including mitochondria, are involved in the production of ROS, such as superoxide anion (O<sub>2</sub><sup>•-</sup>) and hydrogen peroxide (H<sub>2</sub>O<sub>2</sub>). In the case of mitochondria, ROS are an inevitable by-product of aerobic energy production by the respiratory chain and some enzymes of the Krebs cycle. Mitochondria-generated ROS are involved in physiological signaling (Brookes, Yoon, Robotham, Anders, & Sheu, 2004; Droge, 2002; Golubev et al., 2018) and also play a crucial role in mediating tissue injury after ischemia-reperfusion, when tissue oxygen levels are known to change dramatically (Kalogeris, Bao, & Korthuis, 2014; Lust, Taylor, Pundik, Selman, & Ratcheson, 2002). In addition, mitochondrial ROS have been implicated as major players in the tissue reaction to a non-lethal lack of oxygen via stabilization of HIF1 $\alpha$ , a key transcriptional factor governing the tissue hypoxic response (Bell et al., 2007; Guzy et al., 2005; Hoppel, Vogt, Weibel, & Fluck, 2003; Semenza, 2011).

In mitochondria, one-electron oxidation of the reduced redox centers of several enzymes by molecular oxygen results in the production of superoxide anion radical O<sub>2</sub><sup>•-</sup> as a precursor of the other ROS (see Murphy, 2009, for a review). The superoxide anion can be converted non-enzymatically or by superoxide dismutase (SOD) into hydrogen peroxide (H<sub>2</sub>O<sub>2</sub>). In addition, some redox centers, such as reduced or semi-reduced flavins, can react with oxygen to produce H<sub>2</sub>O<sub>2</sub> directly (Esterhazy, King, Yakovlev, & Hirst, 2008; Grivnikova & Vinogradov, 2013).

$\text{H}_2\text{O}_2$  that is produced in mitochondria can diffuse through the inner membrane of the organelle and can be measured spectrophotometrically using coupled assays in the external medium. One of the most convenient methods to measure  $\text{H}_2\text{O}_2$  is based on the stoichiometric conversion of non-fluorescent Amplex UltraRed to fluorescent resorufin by  $\text{H}_2\text{O}_2$  in the presence of horseradish peroxidase (HRP). Resorufin can be measured accurately either by absorbance (at 570 nm) or by fluorescence (excitation/emission of 568/581 nm).

It should be noted that in respiring intact mitochondria, superoxide, and consequently  $\text{H}_2\text{O}_2$ , can be formed both at the matrix side and the intermembrane space side of the inner membrane. Addition of substrates (malate, pyruvate, succinate, etc.) to isolated mitochondria leads to production of ROS by the respiratory chain on both sides of the inner membrane. While  $\text{H}_2\text{O}_2$  in the intermembrane space is readily detected by the Amplex UltraRed/HRP system, the detectability and metabolic fate of  $\text{H}_2\text{O}_2$  produced in the matrix is less clear.  $\text{H}_2\text{O}_2$  that is generated in the matrix can be removed by the ROS-metabolizing enzymes glutathione peroxidases, peroxiredoxins, glutaredoxin, or thioredoxin-dependent peroxide reductases, with their antioxidant activity being NADPH-dependent (Andreyev, Kushnareva, Murphy, & Starkov, 2015). Therefore, after partial depletion of matrix  $\text{H}_2\text{O}_2$ -removal capacity following the initiation of the respiration, a steady-state level of  $\text{H}_2\text{O}_2$  diffusion from the matrix to the outside will be established. Overall, it is crucial to bear in mind that the apparent rate of fluorescence increase measured with the Amplex UltraRed/HRP assay is not equivalent to the “production” of ROS but rather reflects a rate of “release” or “emission” of  $\text{H}_2\text{O}_2$  from mitochondria.

Because oxygen is a precursor for any ROS, mitochondrial ROS production is defined by oxygen availability in addition to the redox state of the respiratory chain enzymes, matrix NAD(P)/NAD(P)H ratio, and membrane potential across the inner membrane. Thus, the development of a mechanistic model of ROS generation in situ requires a quantitative assessment of  $\text{H}_2\text{O}_2$  release from the organelle at varying oxygen tensions. In addition, while ROS release in vitro is usually measured at ambient oxygen tensions (i.e.,  $\sim 200 \mu\text{M O}_2$ ), the concentration of oxygen in tissues such as the brain and heart is much lower (e.g., 20–30  $\mu\text{M O}_2$  at the 1 mm depth in the cortex) (Ndubuizu & LaManna, 2007; Xu, Boas, Sakadzic, & LaManna, 2017). Therefore, the knowledge of the ROS generation rate vs oxygen concentration would enable one to extrapolate known in vitro values to the physiologically relevant settings.

In this chapter, we describe a simple and reliable protocol to measure the dependence of mitochondrial  $\text{H}_2\text{O}_2$  release on oxygen concentration, which we implemented in several of our studies (Jain et al., 2019; Stepanova, Konrad, Guerrero-Castillo, et al., 2018; Stepanova, Konrad, Manfredi, et al., 2018; Stepanova et al., 2019). Our method uses the Oroboros respirometer equipped with a fluorescent module to measure simultaneously oxygen consumption and  $\text{H}_2\text{O}_2$  release with Amplex UltraRed/HRP by mitochondria isolated from mouse brain. However, this method can be applied to any ROS-generating system (microsomes, peroxisomes, activated macrophages, or bacteria), and measured using any conventional respirometer, fluorescent setup and gas delivery system.

### 3 Materials, equipment and reagents

1. *Reagents*: ADP (Sigma A5285), Amplex UltraRed (ThermoFisher A36006), bovine serum albumin (BSA) essentially fatty acid free (Sigma A6003), EGTA (Sigma E3889), glycerol 3-phosphate (Sigma 61668), HEPES (Sigma H4036), hydrogen peroxide (Sigma 216763) horseradish peroxidase (ThermoFisher 012001), KCl (Sigma 746436), K<sub>2</sub>HPO<sub>4</sub> (Sigma P9666), mannitol (Sigma 63559), MgCl<sub>2</sub> (Sigma M9272), rotenone (Sigma R8875), succinate (Sigma S2378), sucrose (Sigma S7903), superoxide dismutase (Sigma S9697), and Tris (Sigma T5941). All aqueous solutions should be prepared using deionized MilliQ (Millipore) water. Pressurized argon or nitrogen should be ultrapure or research grade with <1 ppm of oxygen present.
2. *Mitochondrial preparation*: Intact mitochondria are isolated from mouse brain by differential centrifugation with digitonin treatment, as described previously (Stepanova, Konrad, Manfredi, et al., 2018). The respiratory control ratio (5–6 with succinate/glutamate couple) and specific activity per mg of protein of mitochondria prepared using this method are similar to mitochondria isolated using Percoll gradients (Chinopoulos, Zhang, Thomas, Ten, & Starkov, 2011). However, the yields obtained are greater and the time for isolation is shorter (1.5 h) than those for Percoll gradient-based protocols. All steps are carried out on ice or at 4 °C using pre-chilled solutions. The protocol described below is based on use of mitochondria isolated from one mouse brain from a 8 to 10 week-old C57Bl/6J male mouse (~350mg). The yields are typically approximately 1.5–1.8 mg of mitochondria protein. However, material from several mice can be processed simultaneously.

The forebrain hemispheres of one mouse are excised and placed in ice-cold isolation medium (225 mM mannitol, 75 mM sucrose, 20 mM HEPES-Tris, 1 mM EGTA, 1 mg/mL BSA, pH 7.4). The brain is then transferred to a Dounce homogenizer (15 mL, Wheaton) with a tight pestle (A). 10 mL of the isolation medium is added and the tissue is homogenized with 40 up-and-down strokes. The homogenized tissue is diluted twofold using isolation medium, and subjected to centrifugation at 5900 × g for 4 min at 4 °C. Digitonin (10% solution in DMSO) is slowly added to the supernatant to a final concentration 0.02% with stirring, and the suspension is incubated for 3–5 min on ice. The suspension is then subjected to centrifugation at 10,000 × g for 10 min and the supernatant is discarded. The pellet is resuspended by gentle pipetting in the BSA-free isolation buffer, and washed in the same buffer two times by centrifugation at 10,000 × g for 10 min at 4 °C. At the end of the isolation, the mitochondrial pellet is resuspended in 100 μL BSA-free isolation buffer. Aliquots are taken for protein determination, and the remaining suspension is stored on ice.
3. *Measurement assay medium*: 125 mM KCl, 14 mM NaCl, 0.2 mM EGTA, 4 mM KH<sub>2</sub>PO<sub>4</sub>, 2 mM MgCl<sub>2</sub>, 20 mM HEPES-Tris, pH 7.4, supplemented with 1 mg/mL BSA. Components of the H<sub>2</sub>O<sub>2</sub> measuring system: 10 μM Amplex UltraRed,

4 U/mL HRP, and 40 U/mL Cu/Zn superoxide dismutase are added to the assay medium before the experiment (see Section 6). The assay medium should be kept at 37 °C during the experiment. See also Note 1.

Substrates and effectors working solutions:

1. Succinate, 1 M (water, pH adjusted)
2. Glycerol 3-phosphate, 2 M (water)
3. ADP, 0.1 M (water, pH adjusted)
4. Rotenone (complex I inhibitor), 5 mM in DMSO

### 3.1 Instrumentation

Mitochondrial respiration and H<sub>2</sub>O<sub>2</sub> release are measured using an Oroboros O2k high-resolution respirometer equipped with a two-channel fluorescence optical module (excitation at 525 nm and emission at 580–700 nm) to simultaneously monitor oxygen concentration and a change in fluorescence. We use a home-built optical module (see the details in [Stepanova et al., 2017](#)), but the proprietary sensors are available from Oroboros (#44210-01). Detailed instructions and videos for electrode assembly, chamber volume adjustment, instrumental background correction, oxygen calibration, and DatLab software use can be found at <https://wiki.orooboros.at>.

To study H<sub>2</sub>O<sub>2</sub> release at varying oxygen concentrations, we further developed the Oroboros respirometer to include a gas headspace above the mitochondrial suspension within the measurement chamber. By varying the partial pressure of argon or nitrogen gas in the headspace, one is able to rapidly decrease the oxygen concentration in the liquid sample via gas exchange between the two phases. Our system ([Fig. 1](#)) comprises a respirometer with a Clark-type electrode. Short custom stoppers (plungers) with conical shaft for the Oroboros chamber are 3D printed (Form2, Formlabs, USA) with a Viton O-ring, and contain thin channels to allow gas flow into the headspace (1 mm diameter) and the injection port of reagents into the chamber (0.5 mm diameter).

Oxygen-free gas from a cylinder tank equipped with a standard regulator is fed via 5-mm silicon or PVC tubing to a Cole-Palmer flowmeter, or any other type of gas proportioner. The gas flow rate is typically 20–100 mL/min; however, the optimal rate should be determined for each newly built up system (Steps 1–4 below). The flowmeter is connected to a 150-mL glass washing bottle with a coarse fritted disc (Lenz #5510137); however, any kind of humidifier/washing bottle of 50–200 mL capacity and equipped with porous filter can be used. For humidification, argon is bubbled through 20–30 mL of water in the washing bottle connected via a Y-fork with 1-mm polyethylene tubings to two short custom stoppers above the 1-mL head space.

The oxygen electrode chamber holds 2 mL of mitochondria suspension, but volumes as low as 1 mL can be used. A magnetic stirrer is used to provide even oxygen distribution and to help gas exchange between the gas-liquid interphase. Our system monitors oxygen concentration but not mitochondrial respiration, due to the exchange of oxygen between the medium and the head space.

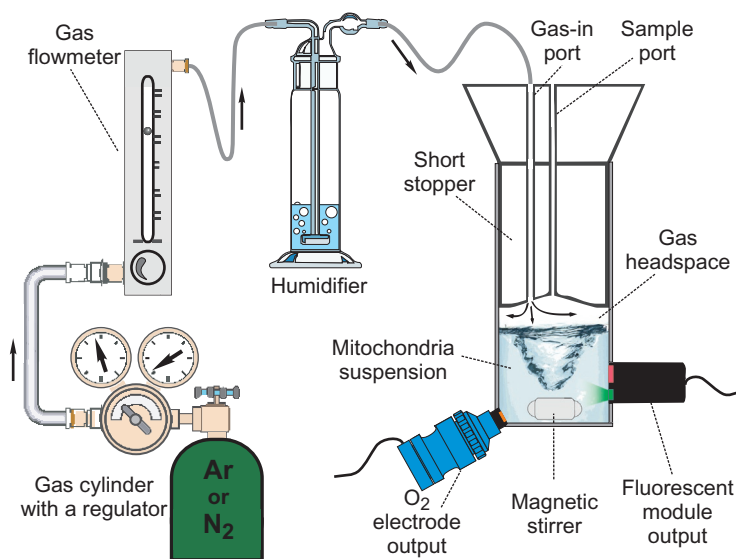
6 Measurement of mitochondrial H<sub>2</sub>O<sub>2</sub> production

FIG. 1

Diagram of the experimental setup. The direction of the gas flow is shown by the black arrows. Fine regulation of the input gas from the cylinder is provided by the gas flowmeter. Gas is humidified in the glass washing bottle prior to entering the chamber headspace via 1-mm tubing through the short stopper. For clarity only one electrode chamber of the Oroboros respirometer is schematically shown. The central sample port also serves as the gas output. Components are not shown to scale. For further details, see main text.

However, since complex IV binds to oxygen with high affinity (apparent  $K_m < 0.4 \mu\text{M O}_2$ ), the rate of respiration by intact mitochondria stays linear until very low oxygen levels ( $2\text{--}4 \mu\text{M O}_2$ ).

The measurements are performed at 37 °C using a stirring speed of 850 rpm, and a time resolution of 0.2 s. The polarization voltage for the oxygen electrodes is 800 mV and the gain for the optical channels is 100. The oxygen solubility factor of the medium (FM value in the DatLab calibration menu) is 0.966. During actual measurements, the chamber lights should be off to avoid interference with fluorescence detection.

*Running time:* Mitochondrial isolation 1 h 30 min; instrument preparation 30 min; time required to run two assays to obtain two sets of data on H<sub>2</sub>O<sub>2</sub> release vs [O<sub>2</sub>] is 5–10 min.

#### 4 Protocol

The Amplex UltraRed/HRP H<sub>2</sub>O<sub>2</sub> detecting system should be tested prior to running experiments with mitochondria by careful titration of the fluorescent signal with small consecutive additions of 100–200 nM H<sub>2</sub>O<sub>2</sub> to obtain a “staircase”-like trace to ascertain a linearity between fluorescence increase and amount of H<sub>2</sub>O<sub>2</sub> added. Please see Note 1.

Prior to the experiments with mitochondria, a test run of oxygen depletion by argon or nitrogen purging should be carried out to check the system performance (Steps 1–4). This will reveal the system's dead time, signal stability, time needed to complete oxygen depletion, and can also be used to calibrate the oxygen electrode signal.

1. Carefully wash the respirometer chambers with water: add 0.5 mL assay medium, aspirate and add 2 mL of pre-warmed (37 °C) assay medium containing all the components except for the Amplex UltraRed/HRP H<sub>2</sub>O<sub>2</sub> measuring system.
2. Insert the short stoppers connected with the argon flowing system. Wait until the basal level is stabilized. This value will be used for Air calibration in the DatLab Calibration menu.
3. Switch on the argon and observe a quick decrease of oxygen in the chamber. At gas flow rates of 30–50 mL/min, it should take 2–5 min to completely displace all oxygen from the solution. Wait until the oxygen signal reaches zero (the oxygen flux should be also close to zero). This value is used for Zero calibration. It is very important to adjust the rate of the gas flow so that the total time for complete displacement of oxygen is not higher than 5 min. See Note 2.
4. Use the obtained Air calibration and Zero calibration levels (DatLab Calibration menu c1 and c0 values, respectively) to accurately set up the correct oxygen scale before the experiments.

After calibration is complete, the experiment can be started using the ROS-generating system. We typically use mitochondria isolated from mouse brain; however, any enzymatic H<sub>2</sub>O<sub>2</sub>-producing system can be tested. Various substrates can be used to initiate respiration associated with H<sub>2</sub>O<sub>2</sub> release. The malate/pyruvate couple is used to generate matrix NADH for respiration by complexes I–II–IV. Pyruvate is oxidized by pyruvate dehydrogenase, generating NADH and acetyl-CoA which further reacts with matrix oxaloacetate and stimulates malate dehydrogenase-catalyzed formation of NADH. Succinate drives the reduction of quinone by complex II, which shuttles electrons to complexes III–IV. Note that oxidation of succinate may lead to the accumulation of the matrix TCA-cycle metabolite oxaloacetate, which is a potent inhibitor of complex II (Stepanova, Konrad, Manfredi, et al., 2018 and references therein). Therefore, when measuring complex II-supported respiration, it is advisable to use succinate in conjunction with glutamate, so that glutamic-oxaloacetic transaminase removes oxaloacetate.

In addition, brain mitochondria possess glycerol 3-phosphate dehydrogenase (the GPD2 isoform) with an activity comparable to that of complex II. This enzyme, located on the intermembrane space side of the inner mitochondrial membrane, converts glycerol-3-phosphate to dihydroxyacetone phosphate, using quinone as an acceptor substrate, and provides electrons to complexes III–IV similar to complex II (Kwong & Sohal, 1998; Patole, Swaroop, & Ramasarma, 1986). During the oxidation of

succinate or glycerol 3-phosphate, the protonmotive force generated by complexes III–IV can drive complex I in the reverse mode, where electrons from ubiquinol are directed upstream to reduce matrix NAD<sup>+</sup>. Reverse electron transfer (RET) provides the highest rate of ROS production in mitochondrial preparations from various sources, including brain (Grivennikova & Vinogradov, 2006; Hinkle, Butow, Racker, & Chance, 1967; Niatsetskaya et al., 2012; Pryde & Hirst, 2011; Quinlan, Perevoshchikova, Hey-Mogensen, Orr, & Brand, 2013; Stepanova, Konrad, Manfredi, et al., 2018; Turrens & Boveris, 1980). H<sub>2</sub>O<sub>2</sub> release in RET was highly sensitive to membrane potential and specific inhibitors of any enzyme of the respiratory chain.

One type of condition can be tested during an experimental run. A single run consists of the addition of fresh mitochondria, followed by addition of substrates of choice, oxygen depletion, and H<sub>2</sub>O<sub>2</sub> signal calibration. Chambers are emptied and carefully washed between runs.

5. Aspirate medium used for the calibration and add 2 mL of new pre-warmed assay medium. Supplement medium with Amplex UltraRed (10 μM), HRP (4 U/mL), and superoxide dismutase (20 U/mL). See Note 3.
6. Add required amount of mitochondria (usually 0.1–0.5 mg protein/mL) using an automatic pipette.
7. Close the chambers with short stoppers connected to the gas flow system.
8. Add respiration substrates through the injection port: (i) 2 mM malate and 5 mM pyruvate, (ii) 5 mM succinate, (iii) 30 mM glycerol 3-phosphate, or a combination of any of these substrates. Depending on the amount of mitochondria used, a limited decrease of oxygen concentration (non-phosphorylating respiration in State 2) and the steady increase of the raw fluorescence signal will occur as a result of resorufin formation due to H<sub>2</sub>O<sub>2</sub> release.
9. Wait until the flux of the fluorescent signal is stabilized (this can take 0.3–3 min, depending on substrate and origin of mitochondria) and then switch on the gas flow. Rapid oxygen depletion will be accompanied with a decrease of the fluorescence rise rate.
10. Wait until the oxygen is completely depleted. This should take no more than 3–5 min. The resulting two traces of [O<sub>2</sub>] in time and fluorescence signal in time will be used for calculation of one set of dependence.
11. Switch off the gas, remove the stoppers on top of the chamber and quickly replace with an Oroboros Cover-Slip lid (#24411-01) or a cap from a 50-mL Falcon tube to prevent admission of ambient light and disturbance of fluorescence signal.
12. Oxygen from the ambient air will diffuse back reaching the basal level of air saturation. This part of the experiment can be also used for further calculations. See Note 4.

Steps 9–12 can be repeated several times; however, it is recommended to use only the first part of the registration curve when oxygen changes from air saturated to zero level. H<sub>2</sub>O<sub>2</sub> calibration should be performed at the end of the run.

13. Wait until the oxygen level has stabilized and add 0.5 mM ADP to ensure the decrease of potential and a dramatic drop in the  $\text{H}_2\text{O}_2$  release rate, so that the rate of fluorescent increase becomes low. ADP addition is not a necessary step but it makes further calculations more convenient and ADP is easily removed when washing the chamber after the experiment is completed. Make 3–4 additions of 3–5  $\mu\text{L}$  of prepared  $\text{H}_2\text{O}_2$  calibration solution, using an automatic pipette and plastic tips (see Precursor preparation). Use fresh tips for each addition. At least 15 s intervals should be kept between additions. Take care to make additions quickly when opening and closing the lid, to reduce the amount of ambient light entering the chamber. The titration should produce a “staircase”-like trace of the raw fluorescent signal over time, with equal increasing “steps” after each addition. If the steps are very different then careful titration of the  $\text{H}_2\text{O}_2$  detecting system of Amplex UltraRed/HRP should be performed (see Note 1).
14. Open the chamber, aspirate the contents, and wash 4–5 times with MilliQ water. If hydrophobic inhibitors or uncouplers are used (rotenone, antimycin, dinitrophenol, etc.), wash with water first, then 4–5 times with 70% ethanol, and then 4–5 times with water.

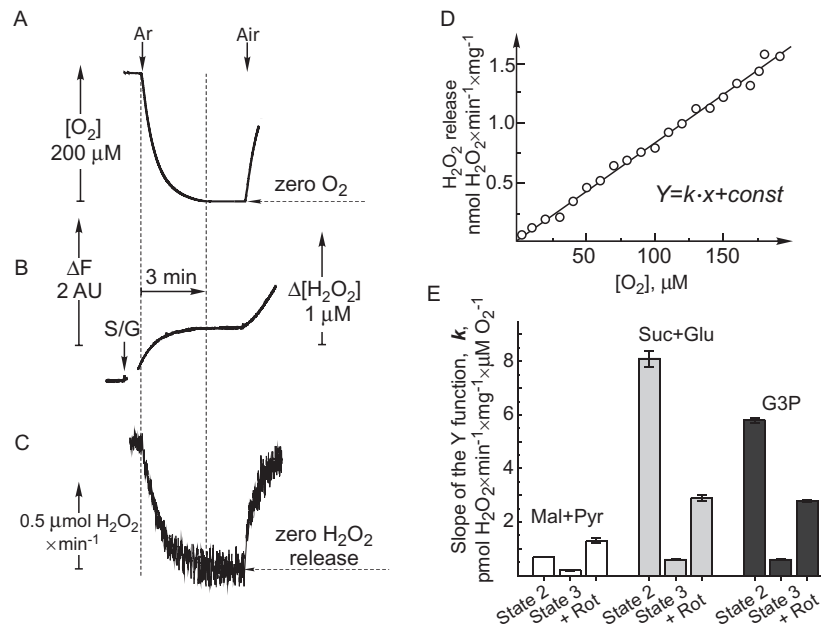
Although the relationship between fluorescence intensity and  $\text{H}_2\text{O}_2$  release is usually unchanged between different runs that use the same conditions (i.e., assay medium, mitochondria and substrate concentrations), the fluorescence signal should be calibrated after each run.

This part of the protocol concludes one run and a set of two time dependences (fluorescent intensity  $F(t)$  vs time and oxygen concentration  $C(t)$  vs time) is obtained that is used for further calculations. For one set of conditions, 5–7 runs must be performed to obtain enough data for statistical analysis.

---

## 5 Analysis and statistics

First, time-courses of fluorescence intensity  $F(t)$  vs time and oxygen concentration  $C(t)$  vs time datasets are generated by DatLab software, using datasets where the oxygen concentration is varied from 200 to 0  $\mu\text{M}$  (Fig. 2A, the part of the trace between the two vertical dashed lines). Depending on the time interval required for the oxygen displacement (3–5 min), each dataset should consist of 1000–1500 time points. The fluorescence intensity change is then converted to  $\text{H}_2\text{O}_2$  concentration change by titrating the fluorescent signal with calibrating solution of  $\text{H}_2\text{O}_2$  at the end of each experiment (Step 13). This calibration can be used to convert fluorescence intensity  $F(t)$  to  $\text{H}_2\text{O}_2$  concentration or ROS( $t$ ) function. DatLab software can plot the derivative of the  $F(t)$  function and this can be used directly to obtain the function of  $\text{H}_2\text{O}_2$  release rate in time ( $d\text{ROS}/dt$ ). Although DatLab software calculates the derivatives of the signals, recordings obtained at 0.2-s collection intervals are too noisy to be used without pre-processing. We obtain better results when the dependence of

10 Measurement of mitochondrial H<sub>2</sub>O<sub>2</sub> production**FIG. 2**

Scheme of a routine experiment for the measurement of the dependence of H<sub>2</sub>O<sub>2</sub> release on oxygen concentration, and data analysis. Representative traces are shown. The reaction is started with the addition of substrates, as shown by the arrow (S/G, 5 mM succinate and 1 mM glutamate) to the assay media containing 0.4 mg/mL mitochondria. The oxygen concentration is measured directly by the Oroboros respirometer (A); the fluorescence signal (B) corresponds to the amount of released H<sub>2</sub>O<sub>2</sub> measured by optical module. The oxygen level decreases rapidly by continuously purging the headspace with argon (Ar). The increase in fluorescence intensity is recalculated to indicate the H<sub>2</sub>O<sub>2</sub> concentration change (B, right) and further into the rate of H<sub>2</sub>O<sub>2</sub> release (C), as detailed in the main text. Only 20 rate points at 20 fixed oxygen concentrations were used for fitting (D). The calculated rates of H<sub>2</sub>O<sub>2</sub> release (circles) were plotted against oxygen concentration and fitted with a linear function Eq. (1) (D) to determine the slope (**k**) of the dependence. The slope of the dependence of H<sub>2</sub>O<sub>2</sub> release rate on the oxygen concentration for different substrates (Mal+Pyr, 2 mM malate/5 mM pyruvate couple; Suc+Glu, 5 mM succinate/2 mM glutamate couple; G3P, 40 mM glycerol 3-phosphate) in respiration state 2 or 3 or in the presence of 1 μM rotenone (E) is indicated. Note that the highest rate of ROS generation (**k**) was found during RET when succinate or glycerol 3-phosphate are oxidized.

Panel E: Adapted from Stepanova, A., Konrad, C., Manfredi, G., Springett, R., Ten, V. & Galkin, A. (2018). The dependence of brain mitochondria reactive oxygen species production on oxygen level is linear, except when inhibited by antimycin A. *Journal of Neurochemistry* 148, 731–745.

$\text{H}_2\text{O}_2$  concentration in time (ROS(t)) is first smoothed and differentiated using available software packages, or manually (see below). We found that a more robust way is to use the original time-course of the Amplex UltraRed fluorescent signal (Fig. 2B), and perform the smoothing, differentiation, and an optional final smoothing, to unify the oxygen concentrations between several experiments using the LOCFIT algorithm (local regression, likelihood and density estimation) (Loader, 1999).

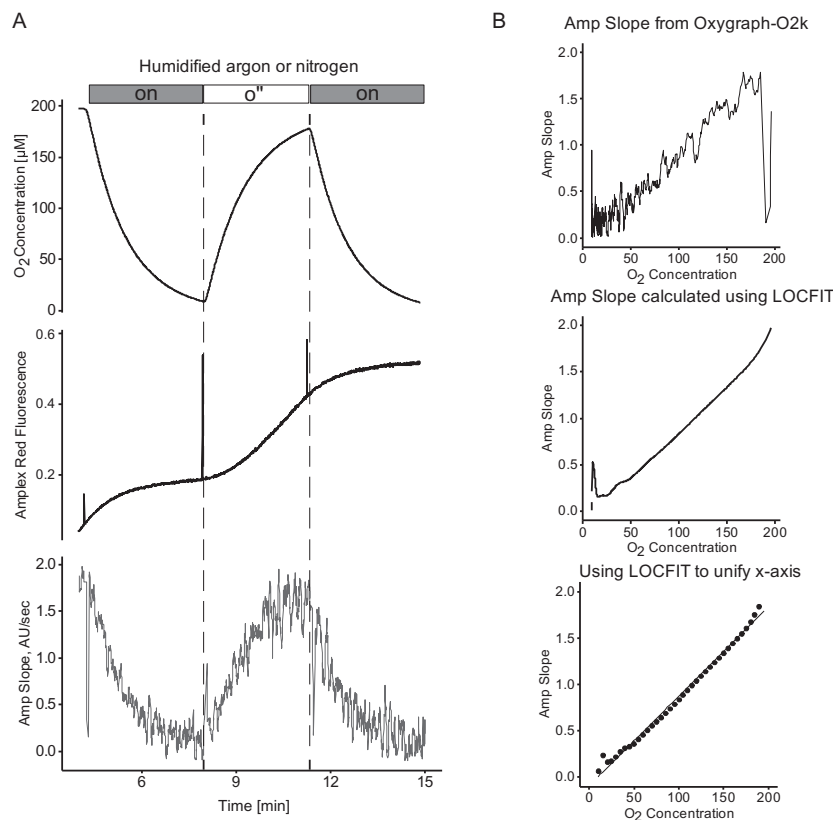
## 5.1 Data analysis algorithm

The initial recording consists of several runs of depletion and restoration of oxygen levels in the chamber (Fig. 3A). The resulting graph is the rate of  $\text{H}_2\text{O}_2$  production plotted against the oxygen concentration. Although Oxygraph-O2k calculates the derivatives of the signals, the recordings at a 0.2-s data collection interval are too noisy to be used without pre-processing (Fig. 3B, compare the top and middle graphs). Use the original time-course of the Amplex UltraRed fluorescent signal (middle graph in Fig. 3A), perform the smoothing, differentiation, and an optional final smoothing to unify the oxygen concentrations between several experiments, using LOCFIT algorithm.

The analysis has been performed using the DatLab to export the data, MS Excel to prepare the data for further analysis, and RStudio (version 1.2.1335 with R version 3.5–3.6) to perform all steps of the analysis and plot the graphs.

### Preparation of the recordings for analysis

- 1) In the DatLab, select File > Export > Data to a text file (\*.csv), then unmark everything but the time (in seconds), oxygen concentration, and Amp signal for a chosen chamber. These columns are the only columns that will be used for further analysis. Each recording may contain several runs of the drop and rise of oxygen levels. Therefore, prior to further analysis, these intervals should be saved separately. For example, the tracing shown in Fig. 3A will be saved in three separate files. See notes A–C below.
- 2) Open the saved .csv file(s) in MS Excel and rename the columns to the abbreviated versions: “T,” “O,” “A” instead of Time (s),  $\text{O}_2$  Concentration (nmol/mL), and Amp ( $\mu\text{M}$ ). One of the reasons for this is that the original names contain some special characters that may be incorrectly interpreted by the program at a later step. Moreover, we recommend that cell A1 should include coded experimental conditions. For instance, “180412.B4: GP40, Rot/0.2Mx” means that the experiment was done on Apr 12, 2018 in chamber B with 40 mM glycerol 3-phosphate in the presence of rotenone, with 0.2 mg/mL of mitochondrial protein. If various conditions are tested, such a system facilitates uniform data storage and analysis.
- 3) Save the prepared file(s) as \*.xlsx in a separate folder. R script was developed in a way to process multiple files at once; for this purpose, each file contains elaborated information, although coded, with the experimental details as described in the previous step.

12 Measurement of mitochondrial  $\text{H}_2\text{O}_2$  production**FIG. 3**

Examples of representative traces and data processing of the results of simultaneous measurement of oxygen concentration and  $\text{H}_2\text{O}_2$  production in isolated mouse brain mitochondria (0.1 mg/mL) respiring on succinate (5mM) to assess the effect of oxygen concentration on the  $\text{H}_2\text{O}_2$  production rate. (A). Traces of oxygen concentration (top), Amplex UltraRed fluorescence (middle)—a measure of  $\text{H}_2\text{O}_2$  release—and the rate of change of the Amplex UltraRed fluorescence (bottom). (B). Examples of plotting the  $\text{H}_2\text{O}_2$  release rate vs oxygen concentration using the data from Oxygraph-O2k (top), using the  $\text{H}_2\text{O}_2$  release rate values calculated from the initial fluorescent data applying The LOCFIT algorithm (middle), or performing an additional adjustment and reduction of the number of points on the x-axis using LOCFIT (bottom).

**Notes on data analysis and fitting**

- A.** Prepare the final dataset using a customized R script. It utilizes .xlsx files formatted according to the recommendations listed above: (a) experimental details in cell A1, (b) three columns named “T,” “O,” “A.” Each dataset consists around 2000 time points. The Amp signal (fluorescent intensity) was smoothed

and differentiated using the LOCFIT algorithm (local regression, likelihood and density estimation) using *locfit* package in R. On the next step, the script performs the reduction of number of points from some 2000 to 20–50. The rationale for this step is that every recording results in a unique set of oxygen levels, thus for the sake of the robust fitting and averaging several datasets, we can define a unified set of oxygen concentrations—the same 20–50 points on the x-axis for all the datasets (bottom graph in Fig. 3B).

- B.** Fit the resulting curves of the H<sub>2</sub>O<sub>2</sub> production rate vs oxygen concentration using a linear function (Eq. 1):

$$y = k \times x + \text{const} \quad (1)$$

where  $y$  is the rate of H<sub>2</sub>O<sub>2</sub> production,  $x$  is the oxygen concentration,  $k$  is the slope of a linear function, and  $\text{const}$  is a fitting parameter (the Y-axis intercept of the linear function). The fitting can be performed using any accessible software or RStudio (`nls` function for non-linear fitting).

- C.** When several datasets for the same conditions are analyzed, different fitting strategies can be implemented: (a) Individual fittings for each dataset followed by finding the averages of all the parameters or (b) averaging the curves before the fitting and finding the weighed fitting. We found that the second approach gives the best fitting (Stepanova et al., 2019).

Each time point of the H<sub>2</sub>O<sub>2</sub> rate (dROS/dt) and oxygen concentration ( $C(t)$ ) function is used to generate a corresponding dataset of dROS/dt vs oxygen concentration. At this stage, it will be clear if the dependence is linear. We detect a linear dependence for the intact brain mitochondria in all tested conditions—any substrate, State 2 or State 3 respiration, the presence of the complex I inhibitor rotenone, the complex III inhibitor myxothiazol, the complex II inhibitor atpenin A5, or the uncoupler SF 6847 (Eq. 1). Therefore, we discuss only a linear fitting below. However, other functions (e.g., hyperbolic) can be used for the fitting if needed (Stepanova, Konrad, Manfredi, et al., 2018).

At least two different approaches to the statistical analysis of the data can be implemented. One is individual fitting for each dataset, where the slopes ( $k$ , in Eq. 1) for every dataset are determined and the average value of  $k \pm \text{SEM}$  is calculated. Alternatively, all data points can be averaged and the resulted mean value for every point is used for the linear fitting, where the resulting SEM is the weighted fitting error (i.e., when the weight of each data point is taken into account, i.e., weighted fitting).

In the second approach, 5–7 datasets of H<sub>2</sub>O<sub>2</sub> rate vs oxygen concentration for a certain condition can be processed for computation. For one dependence, only 20 points are defined by the argument (oxygen concentration) and taken for computation. As a result, 5–7 datasets containing a similar number of data points for comparison can be obtained, and each point can be averaged, plotted and used

for the fitting. In case of clear linear dependence Eq. (1) (above) can be used. In our experience, the best result is obtained with weighted fitting without a constant term ( $const = 0$ , indicating no H<sub>2</sub>O<sub>2</sub> release in complete anoxia). Values of  $k$  in different conditions are compared to estimate the magnitude of H<sub>2</sub>O<sub>2</sub> release.

---

## 6 Precursor techniques

### 6.1 Preparation of components for Amplex UltraRed assay

1. *Amplex UltraRed*. Add 340  $\mu$ L of fresh anhydrous DMSO to 1 mg of Amplex UltraRed (10 mM final concentration). Store this stock solution in 25–50  $\mu$ L aliquots at  $-80^{\circ}\text{C}$  in the dark. Once thawed, the stock solution can be frozen for future use. The Amplex UltraRed solution is clear and should be discarded if it becomes pink.
2. *Horseradish peroxidase*. Dissolve 1000 U of HRP in 1000  $\mu$ L of MilliQ water. Store this 1 U/ $\mu$ L solution in 25–50  $\mu$ L aliquots  $-80^{\circ}\text{C}$ . Any unused solution should be discarded after each experiment.
3. *Superoxide dismutase*. Dissolve 10,000 U of superoxide dismutase in 1000  $\mu$ L MilliQ water. Store this 10 U/ $\mu$ L stock solution in 25–50  $\mu$ L aliquots at  $-80^{\circ}\text{C}$ . Any unused solution should be discarded after each experiment.

### 6.2 Preparation of calibrating H<sub>2</sub>O<sub>2</sub> solution

Solutions of H<sub>2</sub>O<sub>2</sub> should not be handled with Hamilton syringes; plastic tips and automatic pipettes should be used instead. Determine the molar concentration of commercially available 30% solution of H<sub>2</sub>O<sub>2</sub> measuring the UV spectrum at 220–300 nm or the absorbance at 240 nm, using any conventional UV spectrophotometer and quartz cuvette. The extinction coefficient of H<sub>2</sub>O<sub>2</sub> is  $43.6 \text{ M}^{-1} \text{ cm}^{-1}$  at 240 nm (Hildebraunt & Roots, 1975). Zero the baseline using MilliQ water as a reference. Add 50  $\mu$ L of 30% H<sub>2</sub>O<sub>2</sub> to 50 mL of MilliQ water and stir. Add the diluted solution of H<sub>2</sub>O<sub>2</sub> to the empty cuvette and measure the absorbance at 240 nm. A standard 30% solution is approximately 9 M, therefore a 1:1000 dilution would result in an absorbance approximately 0.4 if a standard 1 cm cuvette is used. For example, if the initial 1:1000 dilution gives an absorbance of 0.423 at 240 nm, the concentration of H<sub>2</sub>O<sub>2</sub> in the diluted solution is  $(1000 \text{ mM} \times 0.423)/46.3 = 9.1 \text{ mM}$ . Take 10  $\mu$ L of that solution and add 990  $\mu$ L of MilliQ water to make the working calibrating solution of 91  $\mu$ M. In practice, 50–100  $\mu$ M solutions of H<sub>2</sub>O<sub>2</sub> are convenient to use, so that aliquots of 3–5  $\mu$ L are used for a single calibration step that yields a final concentration of 75–250 nM H<sub>2</sub>O<sub>2</sub> in a 2-mL chamber volume. Keep diluted solutions of H<sub>2</sub>O<sub>2</sub> on ice. The H<sub>2</sub>O<sub>2</sub> calibrating solution must be prepared fresh for each experiment, and is fairly stable for 3–4 h on ice.

## 7 Safety considerations and standards

Rotenone solution is toxic and any contact with skin should be avoided. Use caution when handling DMSO-based stock solutions.

## 8 Pros and cons

Pros	Cons
<p>Excellent technical and educational support for the Oroboros respirometer as well as continuous development of the instrument. Quality control of data reproducibility</p> <p>Accurate, quantitative measurements of dynamic metabolic rates</p> <p>Unlike other available oxygen electrodes, the Oroboros respirometer can be kept assembled and ready for use for months</p> <p>Rapid method (one run can be performed in 5 min)</p> <p>The actual oxygen concentration and oxygen consumption rate are displayed in real-time in the DatLab software</p>	<p>Large sample requirements for a standard setup (but can be decreased to as little as 0.5 mL)</p> <p>Not designed for adhered cells</p> <p>Only two chambers are available. Which is not well suited for high-throughput applications</p> <p>Requires a substantial amount of starting material compared to spectrophotometrical methods or 96-well plate based approaches (e.g., Seahorse)</p> <p>For noisy signals, raw data processing outside DatLab can be performed using more powerful software packages for smoothing and differentiation</p>

### Note 1

More technical details and elaborate explanations of the calibration procedure for the respiration/Amplex UltraRed assay using various mitochondrial preparations can be found in the publications by Gnaiger's group ([Krumshnabel et al., 2015](#); [Makrecka-Kuka, Krumshnabel, & Gnaiger, 2015](#); [Pesta & Gnaiger, 2012](#)), [Starkov \(2010\)](#) as well as previous topics in the present series ([Villani & Attardi, 2007](#)).

### Note 2

If oxygen is not depleted within 3–5 min upon purging with argon, check if (1) the gas flows freely in the system, (2) all connections are tight, and (3) all regulators are open. Sometimes gas exchange can be slowed by the formation of foam on the surface of the mitochondrial suspension. The recommended gas flow rate is 20–100 mL/min, but the exact value depends on the overall geometry and volume of the system. The gas flow should be strong enough to clearly ripple the liquid surface if directed from 1 to 2 cm distance using 1-mm diameter tubing.

## Note 3

The components of the assay (BSA, Amplex UltraRed, HRP, and superoxide dismutase) could be mixed together with measuring medium and added to the Oroboros chamber to save time. The working measuring medium containing all the components should be used within 2–3 h of mixing and the unused solution should be discarded.

## Note 4

Steps 9–12 can be repeated several times, to generate more sets of dependencies. However, the first part of the registration trace when oxygen changes from air saturated to zero level is the only part that should be used.

---

## 9 Alternative methods/procedures

There are several alternatives to our system for the measuring of H<sub>2</sub>O<sub>2</sub> release at varying oxygen concentrations. First, any type of O<sub>2</sub> electrode with a transparent chamber wall can be used (Rank Brothers, Hansatech, etc.). Second, home-built optical models made of commercially available LEDs, photosensitive diodes, and filters connected to a PC via Arduino software (<https://www.arduino.cc/>) can also be used instead of proprietary Oroboros optical sensors. Several home-built systems with a different degree of complexity built on the base of a conventional oxygen electrode have been described (Hollis, Palacios-Callender, Springett, Delpy, & Moncada, 2003; Ripple, Kim, & Springett, 2013; Starlinger & Lubbers, 1973; Unitt, Hollis, Palacios-Callender, Frakich, & Moncada, 2010; Vinogradov & Leikin, 1972).

Another alternative is the use of a conventional fluorospectrophotometer as the base instrument to measure H<sub>2</sub>O<sub>2</sub> release with the Amplex UltraRed/HRP assay, and a miniature O<sub>2</sub> sensor to detect changes in oxygen concentration (Benit et al., 2017; Hoffman, Salter, & Brookes, 2007). There are at least two types of commercially available O<sub>2</sub> sensors that are small enough to be added to the standard fluorescence cuvette: the optical fiber optics O<sub>2</sub>-sensor (World Precision Instruments, Ocean Optics, etc.) or a Clark-type O<sub>2</sub>-microelectrode (ADInstrument, PreSense, Yellow Springs Instruments). Most of the fiber optic sensors are not accurate below 10–20 μM oxygen and O<sub>2</sub>-microelectrodes have relatively long response times (~20 s). It is critical to use an oxygen detector that can accurately measure low oxygen levels with low response time. Fluorimeter-based systems may be preferred over the described system when higher optical resolution/sensitivity and the availability of any excitation/emission wavelengths are required.

## 10 Troubleshooting and optimization

Problem	Solution
Oxygen baseline is drifting or unstable	Bubbles should not be present inside the chamber when it is closed. Assay medium should be equilibrated at the running temperature of the assay
Foam is formed and is hard to remove	Due to the presence of BSA, the medium tends to foam when added to the chamber or during stirring in the chamber. Therefore, BSA should be added to the chamber immediately before closing the chamber and with stirrers off
The H <sub>2</sub> O <sub>2</sub> release rates are low and not sensitive to additions of ADP or uncoupler	Mitochondria are poorly coupled and are not able to maintain membrane potential high enough to maintain maximal level of ROS release. Isolation procedure should be optimized. The most common problems are long preparation time, contaminated glassware, or unadjusted pH of the isolation or assay media
After several measurements mitochondrial respiration decreases or does not show any increase of respiration after ADP addition or H <sub>2</sub> O <sub>2</sub> release during RET	The most common cause of unexpected response is a contamination of the assay medium with hydrophobic effectors (rotenone, uncoupler, etc.) from previous runs. Rinse the chamber with 70% ethanol at least 4 times and 3–4 times with water after each run. Thoroughly rinse and wipe stoppers with 70% ethanol and rinse with water after each run
There is no increase of fluorescence after addition of aliquots of H <sub>2</sub> O <sub>2</sub> for calibration	Calibrating H <sub>2</sub> O <sub>2</sub> solution deteriorated, likely due to contamination. Prepare a fresh solution
Very low sensitivity to calibrating H <sub>2</sub> O <sub>2</sub> additions, and lack of sensitivity of apparent fluorescence increase to the H <sub>2</sub> O <sub>2</sub> -removing enzyme catalase	Mitochondria from some tissues, such as liver, contain a specific carboxylesterase able to catalyze conversion of Amplex UltraRed to resorufin in a non H <sub>2</sub> O <sub>2</sub> -dependent fashion and at relatively high rate (Miwa et al., 2016). This could obscure the actual fluorescence increase due to H <sub>2</sub> O <sub>2</sub> generation. Sensitivity of H <sub>2</sub> O <sub>2</sub> generation to the carboxylesterase inhibitor phenylmethylsulfonyl fluoride (50–100 μM) should be tested prior to working with mitochondria from unfamiliar sources
Noise of optical fluorescent signal is very high	Bubbles or foam are formed in the suspension. Redo the experiment. Stirring speed may be decreased or position of the optical module heads adjusted
Condensation is formed inside the chamber at the bottom surface of the short stopper	Avoid very long incubation of mitochondria suspension at 37 °C during the experiment

---

## 11 Summary

The data on the dependence of ROS release upon oxygen concentration are particularly important for the field of ischemia/reperfusion injury in pathological conditions such as stroke and cardiac infarction. Indeed, there is evidence that reperfusion-induced oxidative stress can be caused by a transient increase of ROS originating in mitochondria (Chouchani et al., 2014; Martin et al., 2019; Stepanova et al., 2017, 2019). Another essential aspect of the interplay between mitochondria, oxygen and ROS is the possible participation of mitochondrial ROS in hypoxic signaling via stabilization of hypoxia-inducible factor HIF-1 $\alpha$  so that ROS generation is increased at lower oxygen levels (Bell et al., 2007; Chandel et al., 1998; Guzy et al., 2005; Hoppeler et al., 2003; Schieber & Chandel, 2014; Semenza, 2011; Vanden Hoek, Becker, Shao, Li, & Schumacker, 1998). While this mechanism is still not completely understood, our recent data, using the procedure outlined in this chapter, offer new insights on the magnitude of mitochondrial ROS generation at different oxygen levels (Jain et al., 2019; Stepanova et al., 2019; Stepanova, Konrad, Guerrero-Castillo, et al., 2018; Stepanova, Konrad, Manfredi, et al., 2018).

---

## References

- Andreyev, A. Y., Kushnareva, Y. E., Murphy, A. N., & Starkov, A. A. (2015). Mitochondrial ROS metabolism: 10 years later. *Biochemistry-Moscow*, *80*, 517–531.
- Bell, E. L., Klimova, T. A., Eisenbart, J., Moraes, C. T., Murphy, M. P., Budinger, G. R., et al. (2007). The Qo site of the mitochondrial complex III is required for the transduction of hypoxic signaling via reactive oxygen species production. *The Journal of Cell Biology*, *177*, 1029–1036.
- Benit, P., Chretien, D., Porceddu, M., Yanicostas, C., Rak, M., & Rustin, P. (2017). An effective, versatile, and inexpensive device for oxygen uptake measurement. *Journal of Clinical Medicine*, *6*, 58. <https://doi.org/10.3390/jcm6060058>.
- Brookes, P. S., Yoon, Y., Robotham, J. L., Anders, M. W., & Sheu, S. S. (2004). Calcium, ATP, and ROS: A mitochondrial love-hate triangle. *American Journal of Physiology. Cell Physiology*, *287*, C817–C833.
- Chandel, N. S., Maltepe, E., Goldwasser, E., Mathieu, C. E., Simon, M. C., & Schumacker, P. T. (1998). Mitochondrial reactive oxygen species trigger hypoxia-induced transcription. *Proceedings of the National Academy of Sciences of the United States of America*, *95*, 11715–11720.
- Chinopoulos, C., Zhang, S. F., Thomas, B., Ten, V., & Starkov, A. A. (2011). Isolation and functional assessment of mitochondria from small amounts of mouse brain tissue. *Methods in Molecular Biology*, *793*, 311–324.
- Chouchani, E. T., Pell, V. R., Gaude, E., Aksentijevic, D., Sundier, S. Y., Robb, E. L., et al. (2014). Ischaemic accumulation of succinate controls reperfusion injury through mitochondrial ROS. *Nature*, *515*, 431–435.
- D'Autreaux, B., & Toledano, M. B. (2007). ROS as signalling molecules: Mechanisms that generate specificity in ROS homeostasis. *Nature Reviews. Molecular Cell Biology*, *8*, 813–824.

- Droge, W. (2002). Free radicals in the physiological control of cell function. *Physiological Reviews*, *82*, 47–95.
- Esterhazy, D., King, M. S., Yakovlev, G., & Hirst, J. (2008). Production of reactive oxygen species by complex I (NADH:Ubiquinone oxidoreductase) from *Escherichia coli* and comparison to the enzyme from mitochondria. *Biochemistry*, *47*, 3964–3971.
- Golubev, A., Hanson, A. D., & Gladyshev, V. N. (2018). A tale of two concepts: Harmonizing the free radical and antagonistic pleiotropy theories of aging. *Antioxidants & Redox Signaling*, *29*, 1003–1017.
- Grivennikova, V. G., & Vinogradov, A. D. (2006). Generation of superoxide by the mitochondrial complex I. *Biochimica et Biophysica Acta*, *1757*, 553–561.
- Grivennikova, V. G., & Vinogradov, A. D. (2013). Partitioning of superoxide and hydrogen peroxide production by mitochondrial respiratory complex I. *Biochimica et Biophysica Acta: Bioenergetics*, *1827*, 446–454.
- Guzy, R. D., Hoyos, B., Robin, E., Chen, H., Liu, L., Mansfield, K. D., et al. (2005). Mitochondrial complex III is required for hypoxia-induced ROS production and cellular oxygen sensing. *Cell Metabolism*, *1*, 401–408.
- Hildebraunt, A. G., & Roots, I. (1975). Reduced nicotinamide adenine dinucleotide phosphate (NADPH)-dependent formation and breakdown of hydrogen peroxide during mixed function oxidation reactions in liver microsomes. *Archives of Biochemistry and Biophysics*, *171*, 385–397.
- Hinkle, P. C., Butow, R. A., Racker, E., & Chance, B. (1967). Partial resolution of the enzymes catalyzing oxidative phosphorylation. XV. Reverse electron transfer in the flavin-cytochrome beta region of the respiratory chain of beef heart submitochondrial particles. *Journal of Biological Chemistry*, *242*, 5169–5173.
- Hoffman, D. L., Salter, J. D., & Brookes, P. S. (2007). Response of mitochondrial reactive oxygen species generation to steady-state oxygen tension: Implications for hypoxic cell signaling. *American Journal of Physiology. Heart and Circulatory Physiology*, *292*, H101–H108.
- Hollis, V. S., Palacios-Callender, M., Springett, R. J., Delpy, D. T., & Moncada, S. (2003). Monitoring cytochrome redox changes in the mitochondria of intact cells using multi-wavelength visible light spectroscopy. *Biochimica et Biophysica Acta*, *1607*, 191–202.
- Hoppeler, H., Vogt, M., Weibel, E. R., & Fluck, M. (2003). Response of skeletal muscle mitochondria to hypoxia. *Experimental Physiology*, *88*, 109–119.
- Jain, I. H., Zazzaron, L., Goldberger, O., Marutani, E., Wojtkiewicz, G. R., Ast, T., et al. (2019). Leigh syndrome mouse model can be rescued by interventions that normalize brain Hyperoxia, but not HIF activation. *Cell Metabolism*, *30*, 824–832.e3.
- Kalogeris, T., Bao, Y., & Korthuis, R. J. (2014). Mitochondrial reactive oxygen species: A double edged sword in ischemia/reperfusion vs preconditioning. *Redox Biology*, *2*, 702–714.
- Krumschnabel, G., Fontana-Ayoub, M., Sumbalova, Z., Heidler, J., Gauper, K., Fasching, M., et al. (2015). Simultaneous high-resolution measurement of mitochondrial respiration and hydrogen peroxide production. *Methods in Molecular Biology*, *1264*, 245–261.
- Kwong, L. K., & Sohal, R. S. (1998). Substrate and site specificity of hydrogen peroxide generation in mouse mitochondria. *Archives of Biochemistry and Biophysics*, *350*, 118–126.
- Loader, C. (1999). Fitting with LOCFIT. In *Local regression and likelihood* (pp. 45–58). New York: Springer-Verlag.
- Lust, W. D., Taylor, C., Pundik, S., Selman, W. R., & Ratcheson, R. A. (2002). Ischemic cell death: Dynamics of delayed secondary energy failure during reperfusion following focal ischemia. *Metabolic Brain Disease*, *17*, 113–121.

- Makrecka-Kuka, M., Krumschnabel, G., & Gnaiger, E. (2015). High-resolution respirometry for simultaneous measurement of oxygen and hydrogen peroxide fluxes in permeabilized cells, tissue homogenate and isolated mitochondria. *Biomolecules*, *5*, 1319–1338.
- Martin, J. L., Costa, A. S. H., Gruszczczyk, A. V., Beach, T. E., Allen, F. M., Prag, H. A., et al. (2019). Succinate accumulation drives ischaemia-reperfusion injury during organ transplantation. *Nature Metabolism*, *1*, 966–974.
- Miwa, S., Treumann, A., Bell, A., Vistoli, G., Nelson, G., Hay, S., et al. (2016). Carboxylesterase converts Amplex red to resorufin: Implications for mitochondrial H<sub>2</sub>O<sub>2</sub> release assays. *Free Radical Biology & Medicine*, *90*, 173–183.
- Murphy, M. P. (2009). How mitochondria produce reactive oxygen species. *Biochemical Journal*, *417*, 1–13.
- Ndubuizu, O., & LaManna, J. C. (2007). Brain tissue oxygen concentration measurements. *Antioxidants & Redox Signaling*, *9*, 1207–1219.
- Niatsetskaya, Z. V., Sosunov, S. A., Matsiukevich, D., Utkina-Sosunova, I. V., Ratner, V. I., Starkov, A. A., et al. (2012). The oxygen free radicals originating from mitochondrial complex I contribute to oxidative brain injury following hypoxia-ischemia in neonatal mice. *Journal of Neuroscience*, *32*, 3235–3244.
- Patole, M. S., Swaroop, A., & Ramasarma, T. (1986). Generation of H<sub>2</sub>O<sub>2</sub> in brain mitochondria. *Journal of Neurochemistry*, *47*, 1–8.
- Pesta, D., & Gnaiger, E. (2012). High-resolution respirometry: OXPHOS protocols for human cells and permeabilized fibers from small biopsies of human muscle. *Methods in Molecular Biology*, *810*, 25–58.
- Pryde, K. R., & Hirst, J. (2011). Superoxide is produced by the reduced flavin in mitochondrial complex I: A single, unified mechanism that applies during both forward and reverse electron transfer. *Journal of Biological Chemistry*, *286*, 18056–18065.
- Quinlan, C. L., Perevoshchikova, I. V., Hey-Mogensen, M., Orr, A. L., & Brand, M. D. (2013). Sites of reactive oxygen species generation by mitochondria oxidizing different substrates. *Redox Biology*, *1*, 304–312.
- Ripple, M. O., Kim, N., & Springett, R. (2013). Mammalian complex I pumps 4 protons per 2 electrons at high and physiological proton motive force in living cells. *Journal of Biological Chemistry*, *288*, 5374–5380.
- Schieber, M., & Chandel, N. S. (2014). ROS function in redox signaling and oxidative stress. *Current Biology*, *24*, R453–R462.
- Semenza, G. L. (2011). Hypoxia-inducible factor 1: Regulator of mitochondrial metabolism and mediator of ischemic preconditioning. *Biochimica et Biophysica Acta*, *1813*, 1263–1268.
- Starkov, A. A. (2010). Measurement of mitochondrial ROS production. *Methods in Molecular Biology*, *648*, 245–255.
- Starlinger, H., & Lubbers, D. W. (1973). Polarographic measurements of the oxygen pressure performed simultaneously with optical measurements of the redox state of the respiratory chain in suspensions of mitochondria under steady-state conditions at low oxygen tensions. *Pflügers Archiv*, *341*, 15–22.
- Stepanova, A., Kahl, A., Konrad, C., Ten, V., Starkov, A. S., & Galkin, A. (2017). Reverse electron transfer results in a loss of flavin from mitochondrial complex I: Potential mechanism for brain ischemia reperfusion injury. *Journal of Cerebral Blood Flow and Metabolism*, *37*, 3649–3658.

- Stepanova, A., Konrad, C., Guerrero-Castillo, S., Manfredi, G., Vannucci, S., Arnold, S., et al. (2018). Deactivation of mitochondrial complex I after hypoxia-ischemia in the immature brain. *Journal of Cerebral Blood Flow and Metabolism*, *39*, 1790–1802. <https://doi.org/10.1177/0271678X18770331>.
- Stepanova, A., Konrad, C., Manfredi, G., Springett, R., Ten, V., & Galkin, A. (2018). The dependence of brain mitochondria reactive oxygen species production on oxygen level is linear, except when inhibited by antimycin A. *Journal of Neurochemistry*, *148*, 731–745.
- Stepanova, A., Sosunov, S., Niatsetskaya, Z., Konrad, C., Starkov, A. A., Manfredi, G., et al. (2019). Redox-dependent loss of flavin by mitochondrial complex I in brain ischemia/reperfusion injury. *Antioxidants & Redox Signaling*, *31*, 608–622. <https://doi.org/10.1089/ars.2018.7693>.
- Turrens, J. F., & Boveris, A. (1980). Generation of superoxide anion by the NADH dehydrogenase of bovine heart mitochondria. *The Biochemical Journal*, *191*, 421–427.
- Unitt, D. C., Hollis, V. S., Palacios-Callender, M., Frakich, N., & Moncada, S. (2010). Inactivation of nitric oxide by cytochrome c oxidase under steady-state oxygen conditions. *Biochimica et Biophysica Acta*, *1797*, 371–377.
- Vanden Hoek, T. L., Becker, L. B., Shao, Z., Li, C., & Schumacker, P. T. (1998). Reactive oxygen species released from mitochondria during brief hypoxia induce preconditioning in cardiomyocytes. *Journal of Biological Chemistry*, *273*, 18092–18098.
- Villani, G., & Attardi, G. (2007). Polarographic assays of respiratory chain complex activity. *Methods in Cell Biology*, *80*, 121–133.
- Vinogradov, A. D., & Leikin, J. N. (1972). Fluorescence of nicotinamide adenine dinucleotides during the active transport of Ca<sup>2+</sup> ions in liver mitochondria. *Journal of Bioenergetics*, *3*, 203–209.
- Xu, K., Boas, D. A., Sakadzic, S., & LaManna, J. C. (2017). Brain tissue PO<sub>2</sub> measurement during Normoxia and hypoxia using two-photon phosphorescence lifetime microscopy. *Advances in Experimental Medicine and Biology*, *977*, 149–153.
- Zuo, L., Zhou, T., Pannell, B. K., Ziegler, A. C., & Best, T. M. (2015). Biological and physiological role of reactive oxygen species—the good, the bad and the ugly. *Acta Physiologica (Oxford, England)*, *214*, 329–348.